

# The Effects of Fastening Strength on the Variation in Stress Free Temperature in Continuous Welded Rail

P.J. Gräbe

University of Pretoria, Department of Civil Engineering, South Africa

[hannes.grabe@up.ac.za](mailto:hannes.grabe@up.ac.za)

D. Jacobs

University of Pretoria and Transnet Freight Rail, South Africa

[dylan.jacobs@transnet.net](mailto:dylan.jacobs@transnet.net)

**Abstract:** Continuous welded rail (CWR) is a fundamental component of any modern track structure and has several advantages over former types of rail joining processes. The reduction in maintenance and related costs has become the most attractive property of CWR while careful monitoring and maintenance of CWR is essential to ensure safe train operations. Management of the stress free temperature (SFT) of any section of CWR is a vital duty of the track maintenance team to prevent rail breaks and lateral buckling that could lead to derailments. Stress free temperature variations are influenced by a number of external factors. This paper describes experimental field and laboratory tests carried out to investigate to what extent the fastening strength would influence the variation in SFT in CWR track on Fist fastenings and two types of pads. The research established a non-linear

relationship between clamping force and rail movement through the fasteners as well as a strongly linear relationship between clamping force and the variation in SFT. It is also demonstrated that although the friction coefficient of the pad has an influence on rail movement through the fastener, the primary factor influencing SFT variations is the clip force. The paper concludes by quantifying the relationship between clamping force and the expected variation in SFT with clear guidelines on the management of the stress free temperature in CWR.

## **INTRODUCTION**

Continuous welded rail (CWR), also referred to as long welded rail, has become synonymous with modern railways since its introduction in Germany during the early 1820's. Today CWR is common on railway lines characterized by high speed, heavy axle loading and/or high annual traffic volume. Manufactured rail lengths are welded together by means of flash-butt or thermit welding equipment to produce long, continuous rail sections that can stretch over hundreds of kilometres [1].

Continuous welded rail has a number of advantages over conventional jointed rail track. CWR reduces track maintenance and increases the service life of track components [2]. Apart from requiring constant maintenance, jointed track limits maximum train speed and therefore reduces the efficiency of the system [3]. There are however several challenges to the use of continuous welded rails. CWR has to be managed in such a way that the potential failures that accompany it, i.e. rail breaks and lateral buckling, do not compromise the safety of the track. This is done by mobilising the weight and stiffness of the track panel, the friction between the

ballast and the sleepers and the resistance provided by the crib and shoulder ballast to reduce the risk of CWR related track failures [4].

CWR theory is based on the calculation or measurement of longitudinal rail stress, the rail temperature and lateral track resistance and stability. The theory enables the calculation of the stress free temperature (SFT), the most important parameter in the maintenance of safe and reliable continuous welded rail [5].

Variations in the SFT of CWR are a challenge for the track maintainer who needs to manage the stresses related to CWR by careful monitoring and destressing. Stress free temperature variations are influenced by a number of external factors that will be discussed later in the paper. The objective of this research is to investigate the effect of clamping force on the stress free temperature variation in CWR track. Historic data, field measurements and laboratory experiments will be presented to establish a framework in which this relationship can be evaluated.

### **STRESS FREE TEMPERATURE (SFT)**

The SFT or neutral temperature is the temperature at which the rail is fastened stress free to the sleepers, i.e. with neither tension nor compression forces in the rail.

The rail force ( $N$ ) due to a temperature increase, is calculated with the following formula [6]:

$$N = EA\alpha\Delta T \quad (\text{Eq. 1})$$

where:

- $E$  = Young's modulus for the rail (N/mm<sup>2</sup>)
- $A$  = total cross-sectional area of the rail (m<sup>2</sup>)
- $\alpha$  = coefficient of expansion (/°C)
- $\Delta T$  =  $T_{neutral} - T_{actual}$  (°C)

The neutral (or stress free) rail temperature ( $T_{neutral}$ ) is therefore the temperature at which the track is neither in compression nor tension. The rail force will then be approximately 0 kN. If the rail temperature ( $T_{actual}$ ) rises above  $T_{neutral}$ , the track will be in compression. This may cause lateral buckling of the track. A decrease in rail temperature below  $T_{neutral}$  will result in overall tension forces in the track. This may cause rail breaks due to longitudinal forces in the rail.

When longitudinal strain in the rail is measured,  $T_{neutral}$  can be calculated with the following equation [7]:

$$T_{neutral} = T_{actual} + \frac{\varepsilon}{\alpha} \tag{Eq. 2}$$

where:

$\varepsilon$  = the measured longitudinal strain in the rail

### **TYPICAL STRESS FREE TEMPERATURE DATA**

SFT will differ from site to site and will also not necessarily remain constant with time. It is therefore paramount that the track maintainer knows what the stress free temperature is at every location on the track and also how the SFT will vary with time. Daily and seasonal changes will have a significant impact on the management

of continuous welded rail. As a result, various methods are used to assess the SFT in CWR by means of non-destructive methods [8].

Figure 1 shows typical data from a longitudinal rail stress measurement station on the Coal line in South Africa for a period of 5 days. Strain gauges are used to measure longitudinal strain in the rails and enable the calculation of other CWR parameters in conjunction with rail temperature measurements. Once the strain gauges are installed, the Lift Frame Method, developed by Van Tonder [7], is used to calibrate the strain gauges that measure the longitudinal rail forces at each of the measurement stations. The Lift Frame Method is used to determine the SFT of the rail and the datum is thus the strain gauge reading recorded for a known SFT value as determined by using the Lift Frame Method. Full details of the equipment and measurement setup at 100 of these stations are available for further reference [9]. Note that tensile stress is positive and compressive stress negative in Figure 1 and all other graphs in this paper.

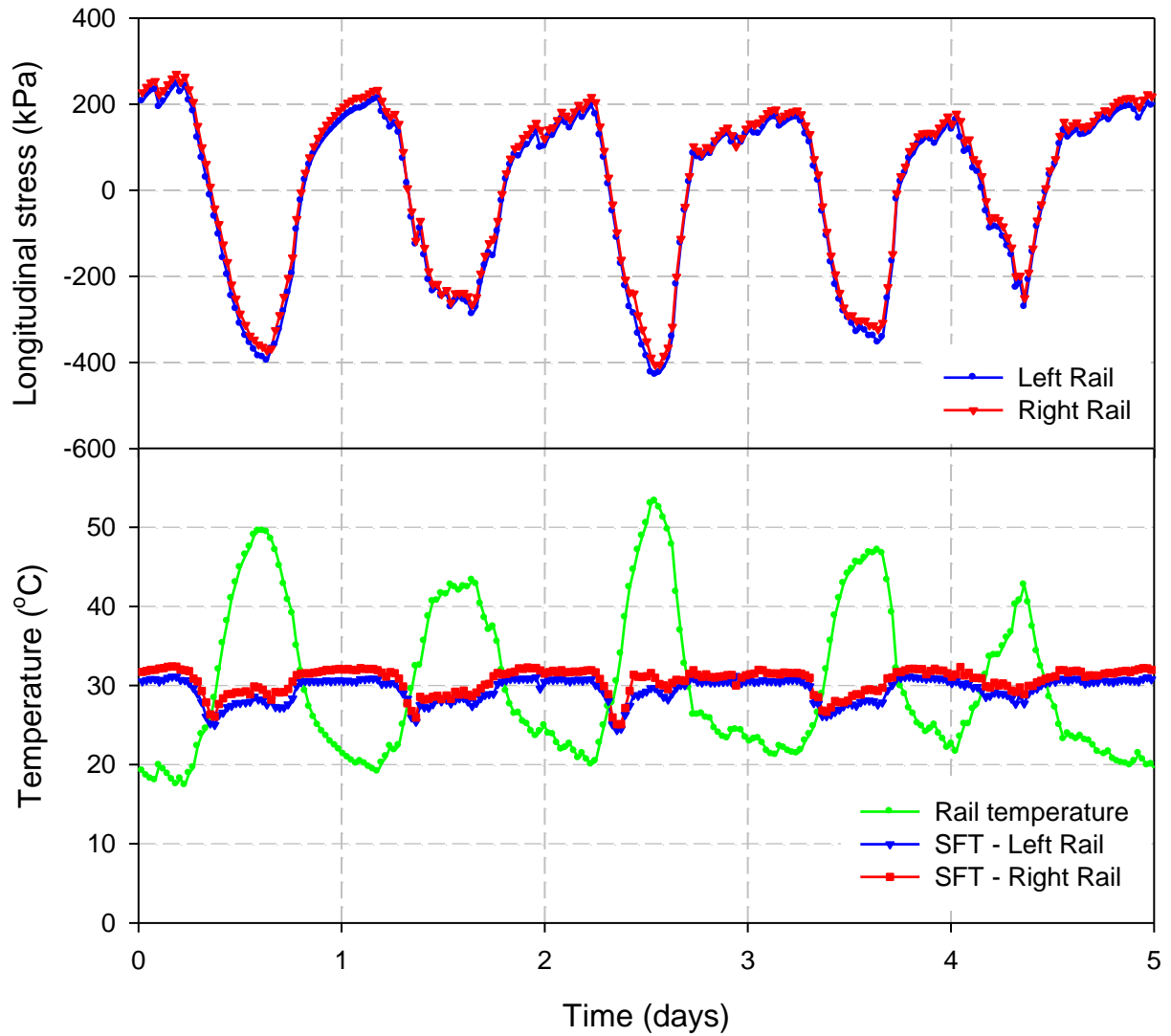


**Figure 1. Typical example of daily variation in stress free temperature.**

The figure clearly illustrates the daily variation in the SFT as well as the accompanying changes in the longitudinal rail stress and rail temperature. The SFT has a range of 7 °C for both the left and the right rails as summarized in Table 1.

**Table 1: Summary of longitudinal rail stress and daily SFT variation**

<b>Parameter</b>	<b>Rail</b>	<b>Minimum</b>	<b>Maximum</b>	<b>Range</b>
Longitudinal stress (kPa)	Left	-424	251	675
	Right	-406	265	671
Stress free temperature (°C)	Left	24	31	7
	Right	25	32	7
Rail temperature (°C)	Both	18	35	17

Figure 2 shows an extract of similar data to those presented in Figure 1, this time for a limited time span of 24 hours only. The figure illustrates the effect of passing trains on the rail temperature as well as the longitudinal rail stress. In this case, passing trains had the effect of raising the rail temperature with between 5 °C and 10 °C. This increase in rail temperature resulted in a reduction in the tension in the rail and would have increased the compression in the rail should the initial rail stress have been negative. Passing trains seem to have a negligible effect on the SFT of the rail. Also demonstrated in the figure are the instances where the rail temperature is equal to the stress free temperature of the rail, clearly coinciding with the two events where the longitudinal rail stress changes from tensile to compressive through zero.

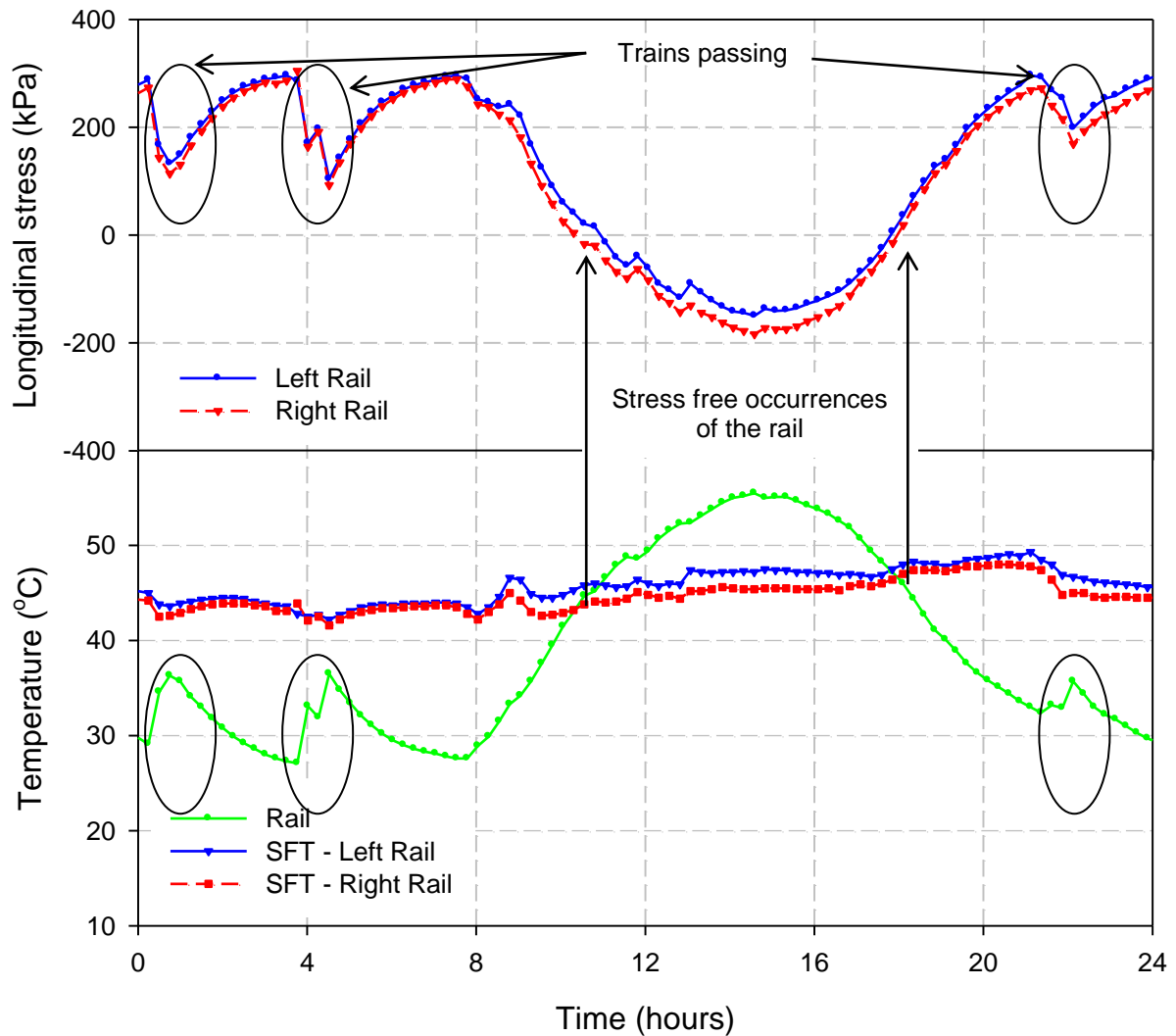


**Figure 2. Typical example of variation in stress free temperature during a 24 hour cycle.**

It was mentioned that the SFT of a section of track does not necessarily remain constant over long periods of time.

Figure 3 shows the gradual drift in the SFT of two rails on a section of track on the Coal line for a 3 month period from December 2010 to March 2011. The daily variation of the SFT is also evident from the scatter of the measurements. Other typical examples, by and large the majority, show constant behaviour over time. It is

however acknowledged that site specific characteristics such as track component condition, track geometry, topography and vehicle loading/braking/acceleration will determine the extent to which the SFT will change, if at all.

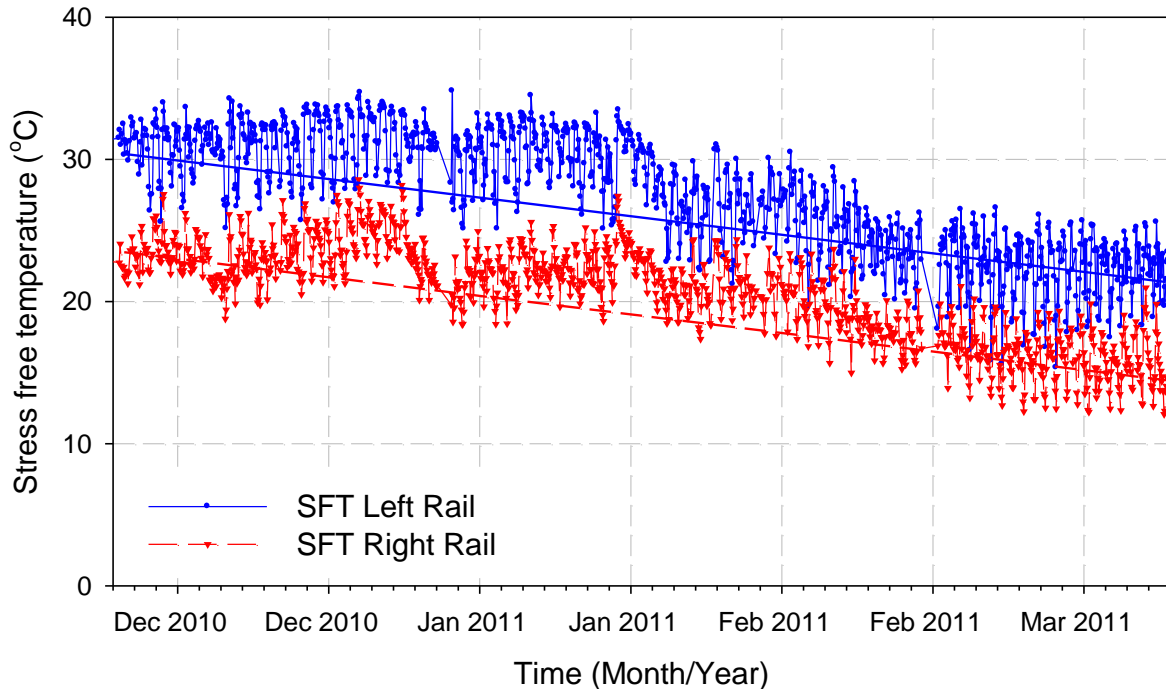


**Figure 3. Typical example of long term drift of the stress free temperature**

## **ASPECTS OF RAIL FASTENERS**

### **Fastening Strength**

It is widely accepted that stress free temperature changes constantly for a given section of track due to the following factors [10]:

- Track maintenance services
- Increased railroad traffic
- Train acceleration and braking forces
- Locations where clips can no longer support the longitudinal forces

- On severe track gradients
- Where there is rail seat erosion and the ballast condition is poor
- As consequences of tamping and ballast cleaning services

The factor in question for this research is the instance where clips can no longer support the longitudinal forces or where the clips allow the rails to move through the fastening systems.

The longitudinal resistance between a rail and sleeper must be at least 15 kN in order for the resistance to be much greater than the longitudinal shear resistance between the sleeper and the ballast. Therefore, when there are large forces within the rail, the fastening system remains in place whilst the sleeper moves within the ballast [6]. The clamping force exerted by the fastening system is extremely important for the transmission of loads to the sleeper. Therefore, a minimum clip force should always be present.

The fastening system is a vital track component which plays an important role in transferring loads between the rail and the sleeper [4]. If the fastening system does not operate efficiently, the rail may absorb more force than desirable and longitudinal movement of the rail through the fastening system may occur. This has an effect on the stress free temperature which could allow it to vary substantially, making it problematic for track maintenance personnel to monitor the rail stresses. It may be expected that the higher the movement through the Fist clip, the higher the variation in stress free temperature will be.

It is known that a fastening arrangement can lose its clamping force with age as well as due to unclipping and clipping when maintenance is carried out. A reduction in the clamping force may allow for an increase in longitudinal movement of the rail through the sleeper as the rail contracts or expands due to changes in rail temperature. It can therefore be hypothesized that the more movement allowed through the fastening system, the higher the variation in stress free temperature would be.

### **Rail/Pad Friction**

An important factor to consider when investigating a rail fastening system is the type of pad used in combination with the other track components. One parameter that needs to be considered when investigating rail pads is the pad friction coefficient that the specific rail pad offers in combination with the rail and the sleeper.

In South Africa, and specifically the heavy haul lines, mainly two different types of rail pads are used, namely HDPE (high-density polyethylene) and Hytrel®, a thermoplastic polyester elastomer. The friction coefficient ( $\mu$ ) of a Hytrel® pad is approximately 0.87 whereas the friction coefficient ( $\mu$ ) of an HDPE pad is approximately 0.69. Static creep resistance tests carried out on the same type of pads revealed that new Hytrel® pads have 23% higher creep resistance than new HDPE pads. For older pads that carried 50 MGT, the figure reduced to 12% [11]. The creep resistance of the pads were determined in a laboratory by measuring the longitudinal force required to initiate slip of a single rail subjected to a static vertical load fastened on two half sleepers. The rail, sleeper and fastener type were kept constant while the pad was changed to measure the creep resistance difference.

The friction coefficient or creep resistance of a rail pad is therefore a vital parameter to consider when investigating rail slip through the fastening system.

Previous work on heavy haul railway lines in South Africa and in the USA [12] has shown that a relatively small amount of movement between the sleeper and the rail is actually required to prevent damage to the track structure as well as skewing of the sleepers. It was concluded that the objective with pad design for heavy haul applications would be to allow for the highest possible elastic displacement of the rail through the fastener without any slip occurring. This objective would be achieved in the case of more elastic rail pads.

The following section describes the research carried out to test the hypothesis that fastening strength would have a significant effect on SFT variations and to determine the relationship between and effect of fastening strength on the variation in SFT.

## **EXPERIMENTAL WORK**

The experimental work carried out as part of this research comprised field and laboratory tests on track components that originated from a specific site on the Coal line in South Africa. The site, instrumentation and different tests are described in the following paragraphs.

### **Site Description**

To conduct the experimental work, five test sites were chosen between Vryheid and Richards Bay on the heavy haul Coal line in South Africa. All five sites had similar

terrain characteristics and the field measurements were all done on Line 1 where trains with fully loaded wagons are operated at a maximum axle load of 26 t.

All sites consisted of the following track components and track structure:

- UIC 60 kg/m rails
- Fist clips
- HDPE or Hytrel® resilient pads
- FY concrete sleepers at a centre to centre spacing of 650 mm
- Heavy haul track substructure consisting of 270 mm – 300 mm ballast, 400 mm subballast and 400 mm selected subgrade material

A typical Fist clip configuration is illustrated in Figure 4.

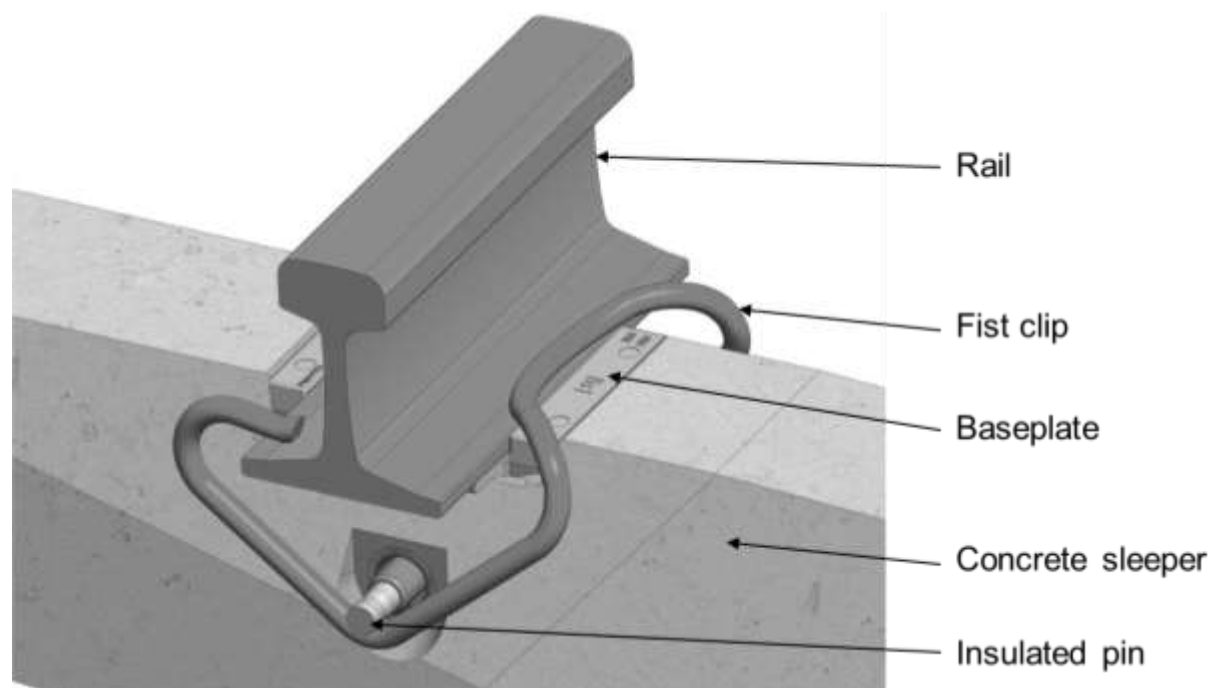


**Figure 4. Typical Fist clip configuration**

## **Instrumentation**

The five test sites used in this research were strategically selected by investigating the variation in stress free temperature as recorded over time by Transnet Freight Rail's WILMA (Wayside Intelligent Longstress Management) system. This system was developed in 2005 to manage continuously welded rails and stress free temperature on heavy haul lines in South Africa. The WILMA system enables the management of CWR by taking rail stress and temperature measurements in real time and can warn track maintenance personnel about possible track buckling due to compression or rail breaks due to tension. The system comprises five different main components namely encapsulated strain gauges, amplifier, communication card, communication interface unit as well as a modem [9].

By calculating longitudinal rail force from strain gauge readings and measuring temperature continuously through the course of the day and sending it to a central file server, it has become a valued system that contributes to the safety and efficiency of heavy haul lines in South Africa.

To determine the stress free temperature (SFT) at each site chosen, WILMA data representative for each of the 5 sites was obtained. By plotting the stress free temperature ( $^{\circ}\text{C}$ ) for these days against time (days) a graph as illustrated in Figure 5 is obtained. Similar graphs for all five sites for the left and right rails were obtained. When analysing a full day, one can observe that during a certain period of the day the stress free temperature remains approximately constant. A similar pattern could be observed for all five days and for each site that was investigated.

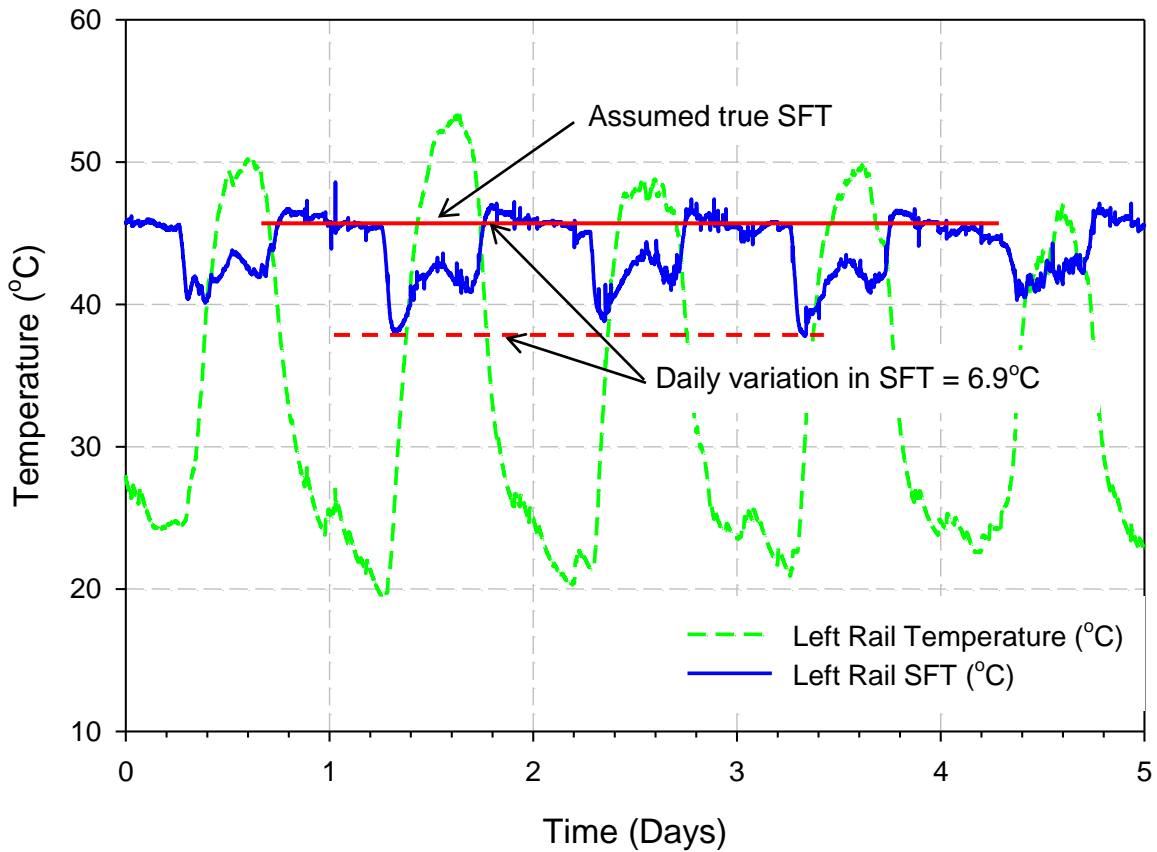


**Figure 5. Typical example of variation in stress free temperature during a 5 day cycle**

From investigating Figure 2 and Figure 5, it is apparent that the “true” stress free temperature stays fairly constant from 18:00 in the evening until 06:00 in the morning. For the other 12 hours of the day the stress free temperature varies through the course of the day in a similar pattern. This is most probably due to the rapid rise in rail temperature up until midday followed by a rapid decrease in temperature as the sun sets, whereas during the night there is not such a fluctuation in temperature. For consistency, the stress free temperature at 03:00 was chosen as the stress free temperature for a specified day. The maximum variation in stress free temperature for each day as well as an average variation in SFT could then be calculated for each site as shown in Figure 5.

Table 2 gives detailed information related to the five test sites used in this study. The SFT Variation ( $^{\circ}\text{C}$ ) represents the average daily fluctuation in the SFT as demonstrated in Figure 5. The stated values are the average values of the left and right rails over a period of 5 days.

**Table 2: Information regarding the various sites use for the experimental setup**

Site	WILMA Station no.	Kilometre Distance/Mast Pole	LVDT Testing	Pad type	Friction Coefficient	SFT Variation ( $^{\circ}\text{C}$ )		
						Left	Right	Avg.
A	18	49/17	Yes	Hytrel	0.87	6.9	7.4	7.2
B	20	53/19	No	Hytrel	0.87	5.2	5.9	5.6
C	23	60/16	Yes	HDPE	0.69	7.6	8.2	7.9
D	28	69/9	No	HDPE	0.69	2.5	3.4	3.0
E	30	71/18	Yes	HDPE	0.69	4.0	3.5	3.8

### Field Tests

Tests were conducted at the 5 different test sites (Sites A, B, C, D and E) over a period of 5 days. At three of the five sites (Sites A, C and E), Linear Variable Differential Transducers (LVDTs) were used to obtain the relative movement of the rail through the fastening system during the course of a single day. An LVDT consists of a movable magnetic core passing through one primary and two secondary coils. Since the core of an LVDT does not contact the coils, friction is avoided. LVDT's are particularly suitable for measuring dynamic motions and very small displacements.

These sites were chosen based on historical WILMA data so that a range of daily SFT variations could be studied. Each setup consisted of 4 LVDTs (L1, L2, R1 and R2) to measure the deflection of the rail relative to the sleeper (see Figure 6).

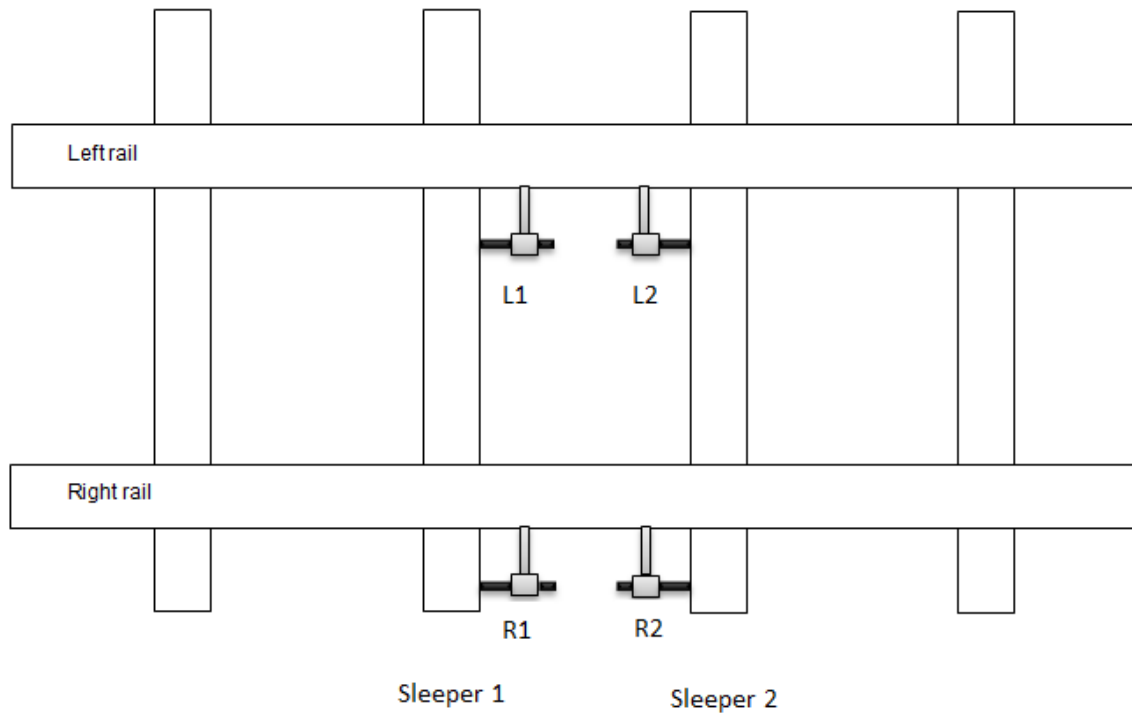


**Figure 6. Setup of LVDTs for deflection measurements on both rails**

Figure 7 illustrates the manner in which each individual LVDT was installed to measure the movement of the rail through the fastening system and relative to the rail.



**Figure 7. Setup of LVDTs for deflection measurement of the rail relative to the sleeper: (a) Site A with instrumentation at 4 fastenings (b) Site A instrumentation at position L2**

The primary reason for not attaching the LVDTs directly onto the fastenings was due to the fact that there was a large amount of vibration in the fastening as compared to the sleeper vibration during the passage of a train.

From the instrumentation described above, the minimum and maximum movement of the rail relative to the sleeper during daily cycles could be obtained together with the corresponding rail temperature as given by the WILMA system (see Figure 8). With this information known, the rate of deflection per unit of temperature could be determined and will be referred to as the rate of rail slip, RS ( $\mu\text{m}/^\circ\text{C}$ ) that occurs through the fastening system.

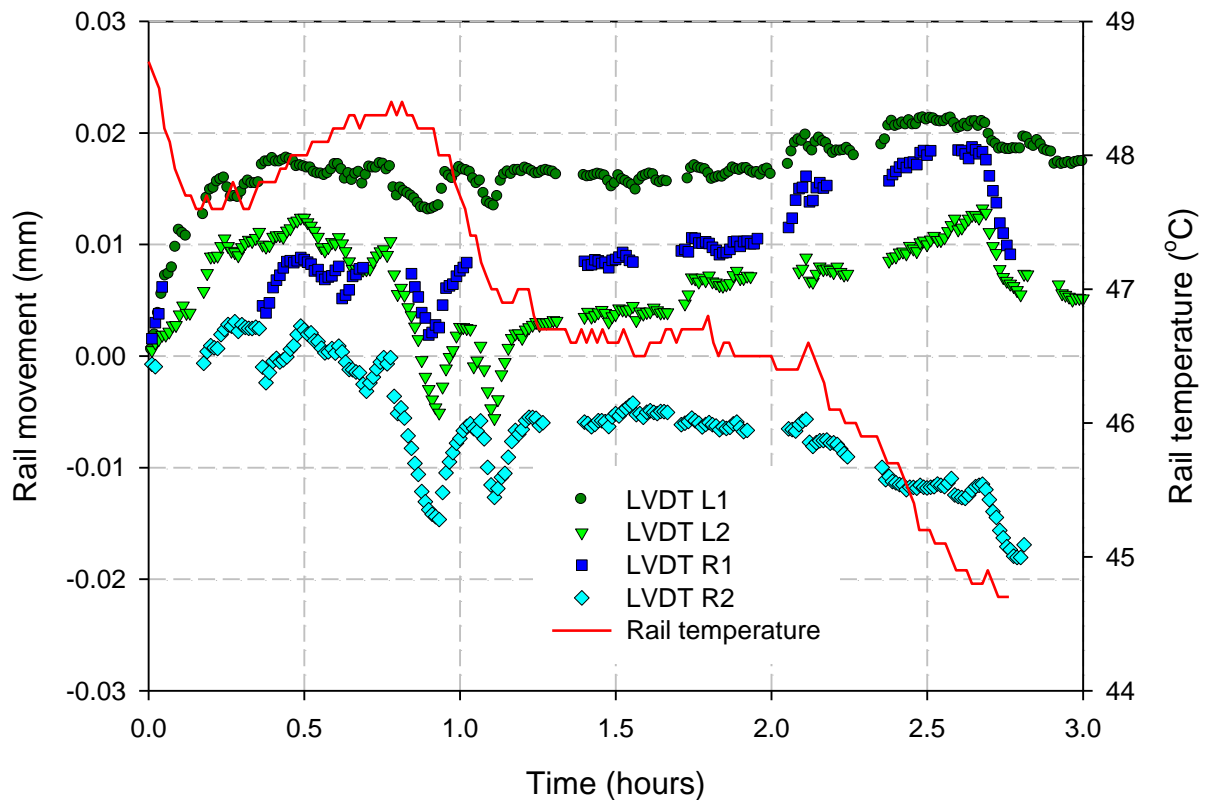


**Figure 8. Example of LVDT deflection measurement of the rail relative to the sleeper (Site A)**

From the graph presented in Figure 8, one can obtain the minimum and maximum deflections, as well as the experimental time at which these values occurred. By using the rail temperature at which the maximum or minimum deflection occurred, the rate of rail slip can be calculated utilizing Equation 3.

$$RS = \frac{|\Delta_{max} - \Delta_{min}|}{|T_{max} - T_{min}|} \quad (\text{Eq.3})$$

Where:

RS = Rail slip rate (mm/°C)

$\Delta_{max}$  = Maximum deflection measured (mm)

$\Delta_{min}$  = Minimum deflection measured (mm)

$T_{max}$  = Temperature corresponding to maximum deflection measured (°C)

$T_{min}$  = Temperature corresponding to minimum deflection measured (°C)

Table 3 reflects the data that was accumulated at each of the three LVDT sites and the average figures that were used in the analysis of the data.

**Table 3: Rail movement through fasteners as a result of temperature changes**

Site	Average variation in SFT (°C)	LVDT	Rail slip rate ( $\mu\text{m}/^\circ\text{C}$ )	Average rail slip rate ( $\mu\text{m}/^\circ\text{C}$ )
A	7.2	L1	6.12	5.05
		L2	3.40	
		R1	5.45	
		R2	5.21	
C	7.9	L1	16.35	15.96
		L2	17.19	
		R1	13.63	
		R2	16.65	
E	3.8	L1	2.72	1.61
		L2	1.09	
		R1	0.83	
		R2	1.79	

## Laboratory Tests

At all 5 measuring sites the Fist fastenings as well as the corresponding pads were removed after completion of the field tests. These fastenings were then taken to a track component laboratory for further investigation and determination of the clamping force of each Fist clip.

All Fist clips were tested on the same testing equipment. The testing procedure is known as the FY Load Testing procedure. The FY represents the type of sleeper size used in conjunction with the Fist clips on heavy haul lines in South Africa.

A metal block was placed underneath the rail to simulate the sleeper used in the field. A pin was fitted through the metal block on which the Fist clip was placed. Once the pin was in place, pin levers were used to install the Fist clips on a UIC 60 kg/m rail. Once the Fist clip was installed, the force which the Fist clip exerts on the flanges of the rail was measured by load cells and displayed on a digital output. The output of the digital reader was in kg force which was then converted to kN for the analysis of the data (see Table 4).

**Table 4: Results obtained from the FY Load Tester**

Site	Fist fastener clamping force (kN)				
	L1	L2	R1	R2	Average
A	24.5	20.2	20.7	18.3	20.9
B	23.9	23.3	22.3	23.4	23.2
C	19.4	21.6	21.6	19.2	20.4
D	26.1	26.4	27.3	20.5	25.1
E	24.5	26.3	23.6	23.6	24.5

The different fastenings and pads were removed from the sleepers as shown in Figure 6, corresponding to the LVDT positions – L1, L2, R1 and R2. A new Fist fastening is expected to have a clamping force of approximately 25 kN.

## DATA ANALYSIS AND DISCUSSION

### Rail slip and variation in SFT

The results obtained from the field experiment and the WILMA data during the time of the field tests, are plotted in Figure 9. The individual measurements from the LVDT's on the left and right rails as well as the calculated SFT values for both rails are presented. The variation in SFT was normalized by dividing through the absolute difference between the maximum and minimum rail temperature during a 24 hour cycle. For all three sites the absolute difference was 30°C.

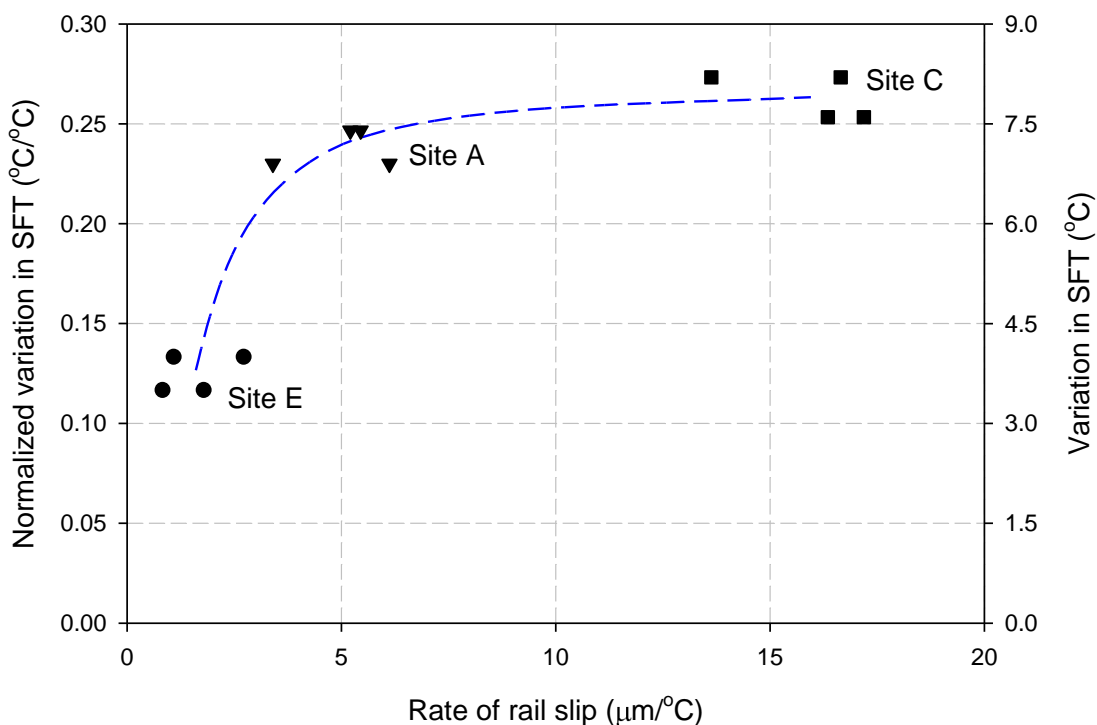


Figure 9. Relationship between rail slip rate and normalized variation in SFT

A clear relationship can be established between the average variation in stress free temperature ( $^{\circ}\text{C}$ ) and the average rate of rail slip ( $\mu\text{m}/^{\circ}\text{C}$ ). An increase in the rate of rail slip allows movement through the fastening system which has been referred to as rail slip. This unrestrained movement of the rail moving through the fastening system causes the SFT to fluctuate as the rail temperature changes. The more rail slip allowed through the fastening system, the higher the resulting variation in stress free temperature. Site C had the highest rate of rail slip of the 3 sites. This caused a high variation in stress free temperature with an average rate of rail slip of  $15.9 \mu\text{m}/^{\circ}\text{C}$ . This is substantially higher (one order of magnitude) than Site E which had an average rate of rail slip of  $1.6 \mu\text{m}/^{\circ}\text{C}$ .

Further investigation of the average variation in SFT of Site A and Site C gives a very similar result for both sites. Site A has an average variation in SFT of  $7.2^{\circ}\text{C}$  whilst the average variation in SFT for Site C is  $7.9^{\circ}\text{C}$ . It is also worth noting that in the laboratory tests Site A and Site C had very similar clip forces ( $20.9 \text{ kN}$  and  $20.4 \text{ kN}$  respectively as shown in Table 4). It should therefore be expected that both sites would have very similar average rates of rail slip. This is however not the case with Site C having an average rate of rail slip 3.2 times greater than the average rate of rail slip for Site A. It can be seen in Table 2 that Site A was fitted with Hytrel pads with a friction coefficient equal to  $0.87$  whilst Site C was fitted with HDPE pads with a friction coefficient of  $0.69$ . It can therefore be concluded that the resisting force in the fastening system is increased as the friction coefficient ( $\mu$ ) is increased for a constant clamping force ( $\text{N}$ ). This provides an explanation to the discrepancy of the average rate of rail slip for Site A and Site C.

Focussing on the results obtained from Site E, it can be seen that the average rate of rail slip is 3.1 times less than the average rate of rail slip at Site A. Site E was fitted with HDPE pads with a friction coefficient of 0.69 whereas Site A was fitted with Hytrel pads with a friction coefficient of 0.87. Although rail slip will be reduced at Site A due to a higher friction coefficient, the rail slip at Site C is still larger than the rail slip at Site E and therefore the average variation of SFT at Site A, which is 7.2 °C, is larger than the average variation of SFT at Site E which is 3.8 °C. This can be explained by referring to the laboratory clip force tests. It is known that the clip force of a new clip is in the order of 25 kN. The average clip force measurement at Site E was 24.5 kN and can therefore be classified as a high clamping force. At Site A the average Fist clip force measurement was 20.9 kN which is substantially lower when being compared to Site E. This large difference in clamping force may be the factor that explains a smaller rail slip at Site E compared to Site A even though Site E had a lower pad friction. It may therefore be deduced from the results that although pad friction is a major parameter influencing the variation in SFT, the force that the Fist clip exerts on the rail will be the dominant parameter with the largest influence on the variation in SFT.

### **Clamping force and variation in SFT**

To study the relationship between the clamping force of the individual fastenings and the variation in SFT, the field test data (Table 3) and laboratory data (Table 4) were combined to produce Figure 10. The figure shows the average variation in SFT as a function of the average clamping force for the five different sites. The clamping forces ranged from 20.9 kN to 25.1 kN which represents the expected clamping force of a new Fist clip (Site D).

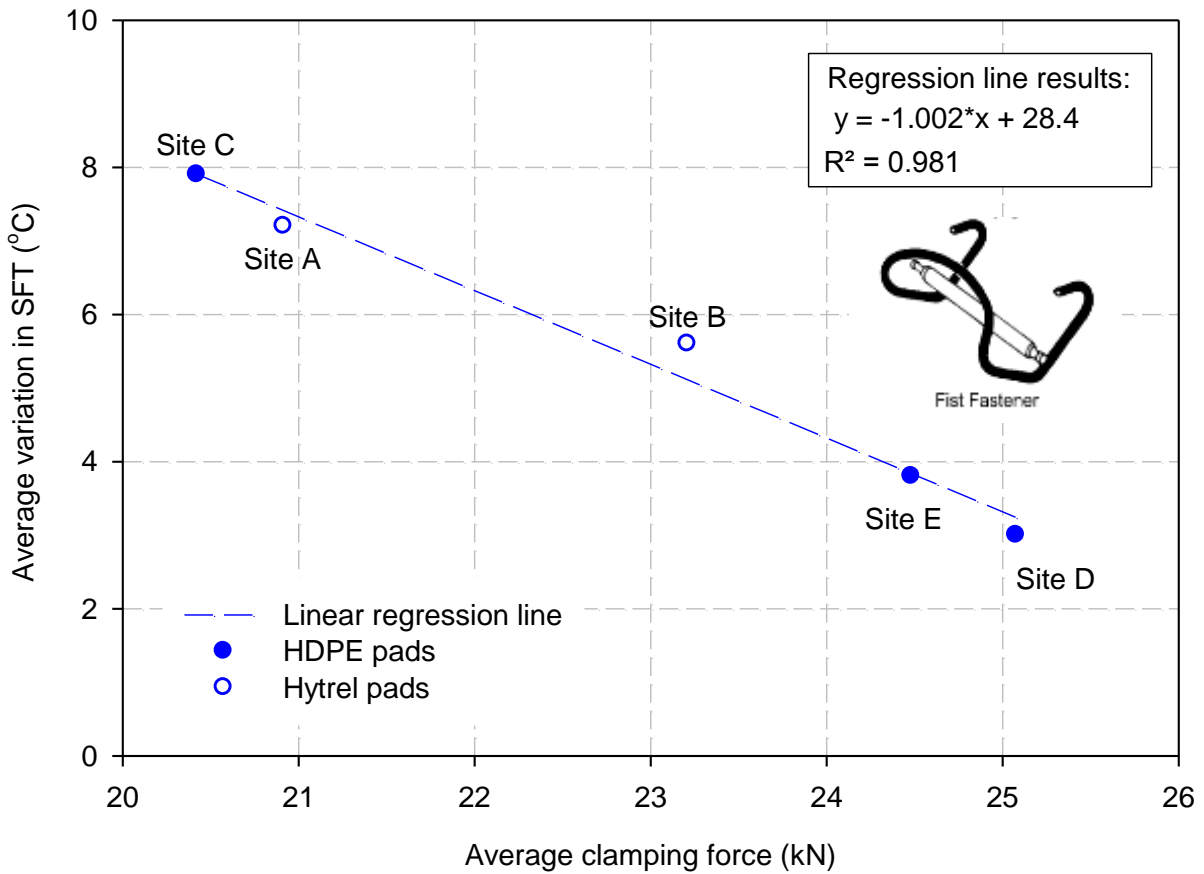


**Figure 10. Relationship between average clamping force and variation in SFT**

As seen in Figure 10, a statistically significant linear relationship was established between the average variation in SFT (°C) and the average clamping force (kN) with a correlation coefficient of 0.981. As the clamping force for the five different sites increases the average variation in stress free temperature decreases.

Referring to Site D it can be seen that the clamping force measurement for this site is relatively high as it has an average clamping force of 25.1 kN. At this value the rail experienced a relatively low variation in SFT of 3 °C. It is noteworthy that Site D was fitted with HDPE pads with a friction coefficient of 0.69. As stated earlier, the pad friction has a significant effect on the variation in SFT. If Site D was fitted with

Hytrel® pads with a friction coefficient of 0.87, a further decrease in the average variation in SFT could have been expected. The fact that the Hytrel® and HDPE data plots on the same linear regression line, supports the notion that clamping force is the decisive factor when considering rail slip and variation in SFT. The friction coefficient of the pad is a secondary factor that can only be mobilized by a high clamping force to reduce movement of the rail through the fastening system.

The regression results indicate that a 1 kN loss in clamping force will most likely result in an increase in SFT variation of approximately 1 °C. A 5 kN decrease in clip force could therefore cause an increase in average variation of SFT of approximately 5 °C. If it is assumed that the normal SFT variation for a new clip is 3 °C, the average SFT variation for a 20 kN clip force will be approximately 8 °C. This conclusion has significant implications for the management of continuous welded rails.

Finally, the average variation in SFT and rate of rail slip are plotted as functions of the clamping force expressed as a percentage of the expected maximum clamping force of a new clip (i.e. 25 kN) for the Fist fastenings that were tested as part of this study (see Figure 11). The non-linear relationship of the rate of rail slip stands in sharp contrast against the linear relationship of the average variation in SFT. Typical values for the rate of rail slip and variation in SFT for new and older fastenings can be deduced from the graph.

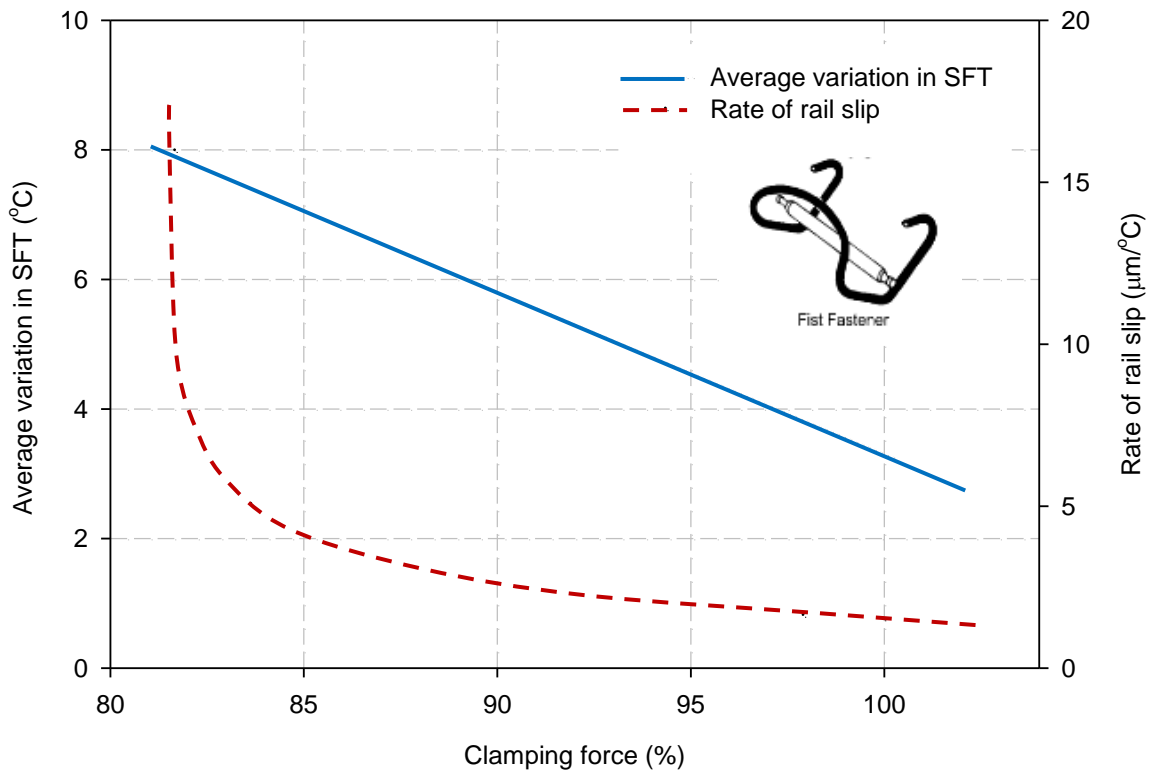


**Figure 11. Relationship between average clamping force, rate of rail slip and variation in SFT**

Figure 11 demonstrates that the rate of rail slip is proportional to the clamping force in the high clamping force space, i.e. 85% to 100%. This relationship is strongly linear until the fastening reaches approximately 85% of its strength where a sudden and sharp increase in the rate of rail slip is observed. Below 85% the slip appears to be relatively unrestrained and high rates of rail slip are recorded. Taking a holistic view, one can deduce that the friction coefficient of the different pads plays a significant role only when the clamping force is high and becomes immaterial when the clamping force is reduced to below 85% of its capacity. A strongly linear relationship between the clamping force and the variation in SFT is however demonstrated over the full range of the clamping force capacity.

## CONCLUSIONS

The objective of this research was to investigate the effect of rail fastening system condition or strength on the phenomenon of varying stress free temperature (SFT). Historical data was presented to illustrate that the SFT of a section of railway track does not necessarily remain constant in the long term and that daily variations in the order of 3 °C to 10 °C are characteristic of most track sections where Fish clips in combination with HDPE or Hytrel® pads are used. It is clear that the fasteners in a rail system have a significant effect on the variation in stress free temperature.

It was demonstrated in the study that the type of pad used in the fastening system has a significant effect on the variation in stress free temperature. By using Hytrel® pads with a friction coefficient of 0.87 compared to HDPE pads with a friction coefficient of 0.69, the variation in stress free temperature can be decreased significantly. The friction coefficient of the pad is however a secondary factor as it can only be mobilized by a sufficiently high clamping force.

In conclusion it can be stated that an increase in the clamping force of the fastening system causes a significant and non-linear reduction in the movement of the rail relative to the sleeper, i.e. the rail slip. As a result of the reduction in rail slip, a decrease in the daily variation of the stress free temperature is also observed. Rail slip is strongly linear in the range of 85% to 100% of the fastening strength, but increases non-linearly below 85% of the fastening strength. In contrast to the non-linear relationship of the rail slip, the variation in SFT relationship is strongly linear.

The daily variation in SFT of a new Fist fastener with a maximum clamping force of 25 kN is in the order of 3 °C. As the clamping force is reduced due to ageing, environmental effects or handling during maintenance, the variation in SFT will increase at a rate of approximately 1 °C/kN. As the variation in stress free temperature increases, it becomes increasingly difficult to manage continuous welded rails as the SFT of the specific track section will vary according to the time and temperature at which the readings are taken. The field measurements indicated that the SFT remains fairly constant when the rail temperature change is a minimum. This experiment was conducted during the night between 18:00 and 6:00. It is therefore desirable to do SFT measurements during these hours if consistent readings are required.

## **ACKNOWLEDGEMENTS**

The following organisations are acknowledged for their contribution towards this research:

- Transnet Freight Rail (TFR) for site access, assistance with field work and permission to use their equipment and facilities. TFR and in particular the Track Testing Centre (Technology Management) is acknowledged for supporting the research activities of the Chair in Railway Engineering at the University of Pretoria.
- University of Pretoria research staff for assistance with the field tests and instrumentation.
- TLC Engineering Solutions for the provision of the WILMA data.
- Pandrol South Africa for the laboratory tests on the Fist fasteners.

This research received no specific grant from any funding agency in the public, commercial, or not-for-profit sectors.

## REFERENCES

1. Lonsdale CP. Thermite Rail Welding: History, Process Developments, Current Practices And Outlook For The 21st Century. In Proceedings of the AREMA 1999 Annual Conference; 1999: The American Railway Engineering and Maintenance-of-Way Association.
2. Lim N, Park H, Kang Y. Stability of Continuously Welded Rail Track. *Journal of Computers & Structures*. 2003 June; 81: p. 2219 - 2236.
3. Sung W, Shih M, Lin C, Go CG. The Critical Loading For Lateral Buckling of Continuously Welded Rail. *Journal of Zhejiang University Science*. 2005 May; 6A(8).
4. Selig ET, Waters JM. *Track Geotechnology and Substructure Management* London: Thomas Telford; 1994.
5. Lombard PC. Continuous Welded Rails. In Proceedings of the 6th 5-Yearly SAICE Conference, 5 - 9 June 1978; 1978; Durban, South Africa: South African Institution of Civil Engineering.
6. Esveld C. *Modern Railway Track*. 2nd ed. Amsterdam, The Netherlands: MRT-Productions; 2001.
7. Van Tonder JPA. *Managing Continuous Welded Rails*. Master's dissertation.

Pretoria, South Africa., Civil Engineering; 1996.

8. Wegner A. Quality Assessment of Continuously Welded Tracks by Nondestructive Testing of Stress-Free Temperature. In Proceedings of the 9th International Heavy Haul Conference; 2009; Shanghai, China: International Heavy Haul Association. p. 198 - 204.
9. Gräbe PJ, Freyer RV, Furno RF. An Intelligent Condition Monitoring System for the Management of Continuously Welded Rails. In Proceedings of the International Heavy Haul Association Conference; 2007; Kiruna, Sweden. p. 579 - 586.
10. Rodrigues, C., Mendonca, C., Jorge, C., Bicalho, B. & Vidon Jr, W. Managing the Rail Thermal Stresses Levels at MRS Tracks – Brazil. In Proceeding of the 9th International Heavy Haul Conference; 2009; Shanghai, China: International Heavy Haul Association. p. 191 - 197.
11. Maree JS. Aspects of resilient rail pads. In Proceedings of the International Heavy Haul Association Conference; 1993; Beijing, China: International Heavy Haul Association. p. 433 - 439.
12. Rhodes, D and Cox, S.J. In Proceedings of the International Heavy Haul Association Conference; 2013; New Delhi, India: International Heavy Haul Association. p. 123 - 126.